

UDC 004.942, 519.635, 519.642, 519.673, 519.652

CC-BY 4.0

## SOFTWARE SYSTEM FOR MATHEMATICAL MODELING THE INFLUENCE OF EFFECTIVE POTENTIALS ON ELECTRON STATES IN QUANTUM WELLS

**Igor Boyko; Sophia Khemii***Ternopil Ivan Puluj National Technical University,  
Ternopil, Ukraine*

**Abstract.** This work presents a detailed review and analysis of mathematical models and development software solutions applicable to the field of electronics of low-dimensional structures. Based on this, the architecture and components of a comprehensive software system were developed, intended for mathematical modeling of the spectral characteristics of electronic states in quantum wells using various effective potentials. A wide range of effective potentials is considered, including: the harmonic oscillator, anharmonic oscillator, Pöschl-Teller potential, modified Pöschl-Teller potential, as well as Morse and Lennard-Jones potentials. Each component of the software system allows users to modify the input physical and geometrical parameters according to the developed mathematical models and the types of functional materials used. In addition, the software enables convenient and efficient visualization of the effective potentials applied to potential wells, performs calculations of electronic spectra dependencies on input parameters, and generates their graphical representations. Based on the developed software modules, a software suite was designed and subsequently constructed in this work for direct application in the fields of nano- and microelectronics, addressing both engineering and purely scientific purposes.

**Key words:** mathematical model, software system, Wolfram Mathematica, quantum well, finite difference method, effective potentials.

[https://doi.org/10.33108/visnyk\\_tntu2025.03.115](https://doi.org/10.33108/visnyk_tntu2025.03.115)

Received 30.07.2025

### 1. INTRODUCTION

In modern electronics, over the last two decades, the field concerning the application of micro- and nanostructures has become significantly widespread. These structures are characterized by their high-tech nature and active connections with other disciplines, especially with the tools and methodologies of information technology.

The aforementioned low-dimensional structures are applied in various human engineering and technological activities, for example, in optoelectronic engineering, semiconductor electronics, and are also of great importance for technologies used in wartime. This is due to the fact that nanodetectors and nanolasers, which are created based on low-dimensional semiconductor structures [1–5], are functional components of equipment designed for detecting the flight of enemy military aircraft (airplanes and UAVs) thanks to the so-called «anti-stealth» technology [6–8].

This is extremely important for the development of Ukrainian science and technology at this difficult time. Another fundamentally different application of this type of structures is found in medicine, where semiconductor lasers are successfully used for performing high-precision operations, especially in oncology, and as a means for effective drug delivery to the necessary location in the human body (so-called effective macromolecules) [9–11].

As for the application of software engineering methods, its subject area is one of the crucial ones when applied to nanoelectronics tasks. This is because, as an analysis of the current state of

technology shows, software systems and complexes support the functioning of electronics components throughout all stages of their lifecycle – starting from their creation and fabrication up to the moment of their direct implementation into specific devices.

Furthermore, the direct functioning of electronic devices based on low-dimensional systems is absolutely impossible without the use of specialized software, which on the one hand ensures the operation itself, and on the other hand, provides the maximum efficiency of these devices.

Software related to nanoelectronics can be categorized into several groups based on its purpose. The first group includes control-type software, which completely controls the process and timeframes during the creation of low-dimensional systems [12–15] based on predefined parameters. Examples of such software systems are software suites supported by the companies Nextnano.de [12–15]. These software suites are multifunctional and are essentially a set of application programs. The complexity of working with such software suites lies in the fact that dozens and hundreds of specialists from software engineering and mathematical modeling can work on each software package, and their subject areas and fields of knowledge may not overlap. This effectively necessitates a completely different approach to the management of such software projects, primarily in terms of work organization. The disadvantages of this group of software systems include the following: their high cost. Even considering the multimillion-dollar expenditures on fabricating low-dimensional structures, purchasing software or ordering specialized software developments from the mentioned companies requires significant financial outlay.

Furthermore, a user can rarely purchase only a specific, required package of programs. Due to the rapid development of this field, the entire software system has to be updated several times a year, but in fact, 90–95% of the software becomes irrelevant and cannot be used anywhere. This constitutes a serious problem and requires a different approach to controlling the development processes of such software.

Thus, for the implementation of such mathematical models, a holistic approach is required, which should ultimately be presented in the form of a complex software system. Each of its software components is responsible for visualizing the potential and implementing the mathematical model itself.

As a result, the findings representing the practical part of this work are as follows. Mathematical models of various effective potentials have been developed, and their visualization has been carried out using the Wolfram Mathematica environment with the help of software components allowing for the change of their main parameters. These software blocks from the first part of the developed software system.

For the second block of the software system, based on mathematical models of boundary value problems with various effective potentials for the Schrödinger equation, their finite difference schemes have been constructed and their software implementation has been carried out. Each component of this software block provides mathematical modeling of the spectrum, localization, and distribution of quasiparticle states by changing the parameters of potential wells, all parameters of effective potentials, and the physical parameters of the materials used.

A flexible architecture has been developed for this software system, which provides clear and fully visualized access to graphical and numerical information obtained from each of the models constructed. By design, the software system will find application both in the field of electronics and in related and interdisciplinary fields, such as the use of microporous materials in air purification systems and the monitoring of harmful emissions into the atmosphere.

## 2. CONSTRUCTION OF A MATHEMATICAL MODEL FOR TASKS DESCRIBING THE OPERATION OF NANOELECTRONICS DEVICES, THEIR NUMERICAL AND SOFTWARE IMPLEMENTATION

Mathematical models used in nano- and microelectronics tasks are typically based on the capability to calculate the electron spectrum. Such models are mainly based on finding analytical or numerical solutions to the time-independent or time-dependent Schrödinger equation. The adequacy of these mathematical models is determined by the fundamental principles of quantum mechanics.

The non-parabolic stationary Schrödinger equation is used in almost all calculations of the band structure of nanodevices with quantum wells. For semiconductor lasers, considering deviations of the quantum well profile from rectangular is of great importance, because a large band gap in quantum wells leads to states located high above the conduction band edge, where this effect becomes noticeable and crucial. This deviation necessitates the construction of separate mathematical models for each case. This modification of the mathematical model can be introduced by introducing a local effective mass for the electron according to relation [16]:

$$m(E, z) = m(z) \{1 + \alpha(z)(E - U(z))\}^{-1}, \quad (1)$$

where  $m$  – the effective mass of the electron in the local region, the model fitting parameter,  $E$  – the electron spectrum energy. Special attention should be paid to the dependence  $U(z)$ , which is a key problem in optimizing the mathematical model and calculating activation energies. The better this function is chosen under the given conditions, the more accurately the activation energies will be calculated, as well as the wave functions of an electron, another quasiparticle or a molecule in general. In the general case, the function  $U(z)$  is also called the model potential. We use two approaches to describing the model potential outside the local region with width  $w$ . In the first, simplified approach, the potential outside the region is infinite, i.e. (Fig.1 a):

$$\begin{matrix} U(z) = U(z) \rightarrow \infty \\ z \rightarrow 0 \quad z \rightarrow w \end{matrix} \quad (2)$$

In such a case, the Schrödinger equation is significantly simplified, and it is often even possible to obtain its analytical solutions. However, such mathematical models provide only qualitatively reliable quantitative results.

In the second approach, the potential outside the local region is considered finite (Fig.1b), that is:

$$\begin{matrix} U(z) = U(z) \rightarrow U_0 \\ z \rightarrow 0 \quad z \rightarrow w \end{matrix} \quad (3)$$

or

$$\begin{matrix} U(z) \rightarrow U_1; U(z) \rightarrow U_2 \\ z \rightarrow 0 \quad z \rightarrow w \end{matrix} \quad (4)$$

Such mathematical models are more realistic. However, they can primarily be implemented numerically, and such an implementation itself requires the use of specialized software or its custom development for such specific tasks.

The initial model considers a single potential well with arbitrary geometric confinement of its base. It is assumed that the potential energy of the electron in the quantum well is determined by its confinement, which is represented by a coordinate dependency  $U=U(z)$ , as shown in Fig. 1 a, b. Accordingly, a simplified model of the local region of the potential well can be obtained from the model in Fig. 1 a when  $U(z)_{z \rightarrow 0} \rightarrow \infty$ ;  $U(z)_{z \rightarrow w} \rightarrow \infty$ . This model represents a potential well that has infinitely high walls. The geometric scheme of such a local region is presented in Fig. 1 b. In both possible models, it is assumed that the potential well has the same width equal to  $w$ .

For this given local region, the determination of the electron spectrum, activation energy, and electron wave functions reduces to finding the solutions of the time-independent Schrödinger equation:

$$H(z)\Psi(z) = E\Psi(z), \quad (5)$$

where the Hamiltonian for the electron in this mathematical model, in the Luttinger modification, is as follows:

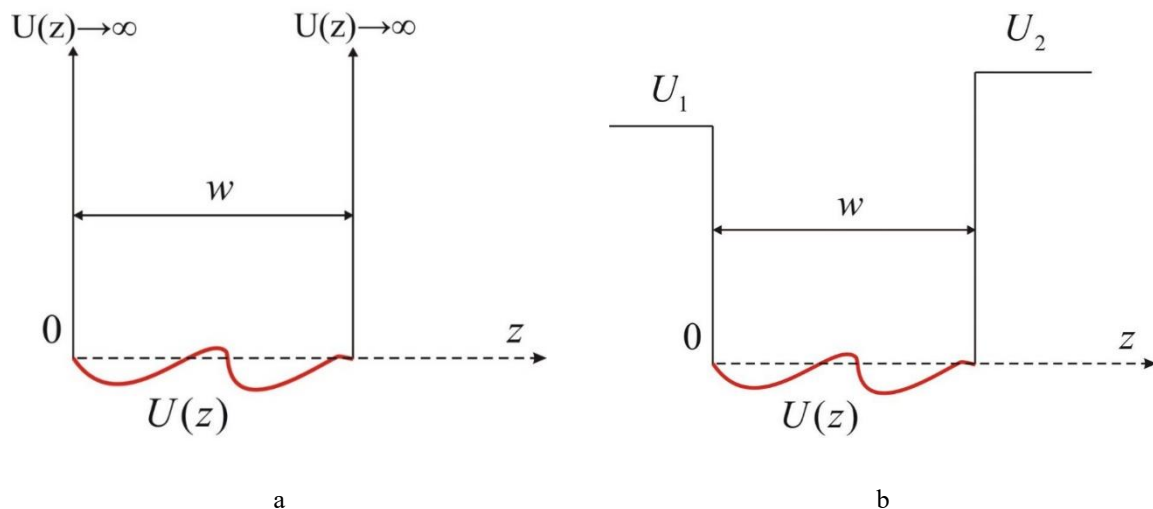


**Figure 1.** Geometric confinement and energy scheme of a potential well with walls of infinite height (a) and with walls of finite height (b)

$$H(z) = -\frac{\hbar^2}{2} \frac{d}{dz} \frac{1}{m(z)} \frac{d}{dz} + \tilde{U}(z), \quad (6)$$

In our mathematical model, it is assumed that the electron has different effective masses in the studied local region and the surrounding medium. This leads to a coordinate dependence of the effective mass  $m(z)$  and the electron's potential energy, which in our case, taking into account the notations used in Fig. 1a, b, are as follows:

$$m(z) = \begin{cases} m_0, & 0 \leq z \leq w, \\ m_1, & z < 0, z > w \end{cases}; \quad \tilde{U}(z) = \begin{cases} U(z), & 0 \leq z \leq w, \\ U_1, & z < 0, \\ U_2, & z > w. \end{cases} \quad (7)$$

When considering expressions (7), the Schrödinger equation is somewhat simplified, and its form for the entire local region will be as follows:

$$\begin{cases} -\frac{\hbar^2}{2m_1} \frac{d^2\Psi(z)}{dz^2} + U_1\Psi(z) = E\Psi(z), & z < 0, \\ -\frac{\hbar^2}{2m_0} \frac{d^2\Psi(z)}{dz^2} + U(z)\Psi(z) = E\Psi(z), & 0 \leq z \leq w, \\ -\frac{\hbar^2}{2m_1} \frac{d^2\Psi(z)}{dz^2} + U_2\Psi(z) = E\Psi(z), & z > w. \end{cases} \quad (8)$$

The requirement for the wave function to be finite expresses the need for the electron to be localized in the studied region with the greatest probability. Specifically, for the mathematical model, this is expressed as the wave function normalization condition:

$$\int_{-\infty}^{+\infty} |\Psi(E, z)|^2 dz = 1 \quad (9)$$

and also, its asymptotics at a significant distance from this local region:

$$\Psi(E, z) \rightarrow 0 \quad z \rightarrow \pm\infty \quad (10)$$

Solutions of the Schrödinger equation in the external environment with respect to the local region can be obtained in exact analytical form. They have the following form:

$$\Psi(z) = A_1 e^{-\chi_1 z} + B_2 e^{\chi_1 z}, \chi_1 = \frac{\sqrt{2m_1(U_1 - E)}}{\hbar}, z < 0. \quad (11)$$

$$\Psi(z) = A_3 e^{-\chi_2 z} + B_3 e^{\chi_2 z}, \chi_2 = \frac{\sqrt{2m_1(U_2 - E)}}{\hbar}, z > w \quad (12)$$

Considering the asymptotics of the wave function given by relations (8), we must consider that the wave function must be finite at  $z < 0$  and  $z > w$ . This leads to the fact that in the expressions for the wave function (11), (12), we must accept  $A_1 = 0$  and  $B_3 = 0$ . As a result, finally for the wave functions in the external region we have:

$$\Psi(z) = B_2 e^{\chi_1 z}, z < 0; \Psi(z) = A_3 e^{-\chi_2 z}, z > w \quad (13)$$

For the wave function in the local region under study, in both mathematical models, which correspond to Fig. 1a, b, boundary conditions must be satisfied, which are responsible for the finiteness of the wave function and the continuity of its probability flow. These boundary conditions are as follows:

$$\begin{cases} \Psi(z)_{z \rightarrow -0} = \Psi(z)_{z \rightarrow +0}; \\ \frac{d\Psi(z)}{dz} \Big|_{z \rightarrow -0} = \frac{d\Psi(z)}{dz} \Big|_{z \rightarrow +0}; \end{cases} \quad \begin{cases} \Psi(z)_{z \rightarrow w-0} = \Psi(z)_{z \rightarrow w+0}; \\ \frac{d\Psi(z)}{dz} \Big|_{z \rightarrow w-0} = \frac{d\Psi(z)}{dz} \Big|_{z \rightarrow w+0}. \end{cases} \quad (14)$$

Conditions (14) lead to a dispersion equation that has transcendental form. His solutions determine the spectrum of an electron, which is in local area is not acquired discrete values:  $E_n$ ,  $n = 1, 2, 3, \dots$ . As a result, the energy value activation is defined as follow:  $\Delta E_{nm} = E_m - E_n$ ,  $m > n$ .

### 3. DEVELOPMENT OF A FINITE DIFFERENCE SCHEME FOR A MATHEMATICAL MODEL WITH THE STATIONARY SCHRÖDINGER EQUATION AND ITS REPLACEMENT BY A GRID PROBLEM

In quantum mechanics, any equation must be modified to conform to the requirements of wave theory, i.e. the electron becomes a wave (particle-wave), so the state of the particle must be given by appropriate boundary conditions. Thus, the new representation of the Schrödinger equation fully describes the peculiar waves corresponding to the particle. The Schrödinger equation, in the one-dimensional case, together with an arbitrary potential  $V(z)$  has the following form:

$$H(z)\Psi(z) = \left[ -\frac{\hbar^2}{2m} \frac{d^2}{dz^2} + V(z) \right] \Psi(z) = E\Psi(z), \quad (15)$$

in this rearrangement it is convenient for us to approach the construction of the difference scheme of this equation. In the relation (15)  $V(z)$  is the potential in which the wave arises;  $H$  – is the Hamiltonian of the problem, analogously to (8), and  $\Psi(z)$  is the wave function or the state of the particle-wave. In the equation (15) the energy  $E$  was defined arbitrarily, that is, it can be any value. As described above, the wave must satisfy the boundary conditions that determine the spectrum of values of  $E$ . Such an equation is called we will call it an eigenequation. Thus, the wave function obtained as a solution of (15) is the actual eigenstate of the particle, respectively, the energy held is the eigenenergy. In matrix terminology, the eigenvector and the eigenvalue are often used as corresponding to the eigenstate and the eigenenergy, respectively.

Let us find out how the boundary conditions determine the eigenenergies for the one-dimensional Schrödinger equation. Any differential operator can be approximated by a finite difference form, so this method is called the finite difference method. For example, if a continuous variable  $x$  is discretized into a series of uniformly distributed points  $x_i$  such that  $x_i = x_0 + i\Delta$  ( $i = 0, 1, 2, \dots, N$ ;  $\Delta$  is a constant – the grid step), then the second derivative is approximated as follows:

$$\frac{d^2}{dx^2} f(x_i) = f''(x) \approx \frac{f(x_{i-1}) - 2f(x_i) + f(x_{i+1})}{\Delta^2}. \quad (16)$$

Then, from equation (15) and considering (16), we easily obtain a set of one-dimensional equations determined by the grid nodes  $x_i$ :

$$\begin{aligned} a(\Psi_2 - 2\Psi_1 + \Psi_0) + V_1\Psi_1 &= E\Psi_1; \\ a(\Psi_3 - 2\Psi_2 + \Psi_1) + V_2\Psi_2 &= E\Psi_2; \\ &\dots \\ a(\Psi_N - 2\Psi_{N-1} + \Psi_{N-2}) + V_{N-1}\Psi_{N-1} &= E\Psi_{N-1}, \end{aligned} \quad (17)$$

where:  $V_i = V(x_i)$ ,  $\Psi_i = \Psi(x_i)$ , and  $a = -\hbar^2 / 2m\Delta^2$ .

For every mathematical model of the local zone, boundary conditions are very important. In the simplest mathematical model, we assume that the wave function is zero both in the leftmost and rightmost coordinates of the local region, i.e.  $\Psi_0 = \Psi_N$ . Then all these equations (17) can be directly presented in matrix form as follows:

$$\begin{pmatrix} -2a + V_1 & a & 0 & 0 & 0 & \dots & 0 \\ a & -2a + V_2 & a & 0 & 0 & \dots & 0 \\ 0 & a & -2a + V_3 & a & 0 & \dots & 0 \\ 0 & 0 & a & -2a + V_4 & a & \dots & 0 \\ \vdots & \vdots & \vdots & \vdots & \vdots & \ddots & \vdots \\ 0 & 0 & 0 & 0 & 0 & \dots & -2a + V_{N-1} \end{pmatrix} \begin{pmatrix} \Psi_1 \\ \Psi_2 \\ \Psi_3 \\ \Psi_4 \\ \vdots \\ \Psi_{N-1} \end{pmatrix} = E \begin{pmatrix} \Psi_1 \\ \Psi_2 \\ \Psi_3 \\ \Psi_4 \\ \vdots \\ \Psi_{N-1} \end{pmatrix} \quad (18)$$

Thus, the finite-difference scheme (2.14) for the mathematical model of the Schrödinger equation is equivalent to the problem of finding the eigenvalues of the matrix

$$A_{nm} = \begin{pmatrix} -2a + V_1 & a & 0 & 0 & 0 & \dots & 0 \\ a & -2a + V_2 & a & 0 & 0 & \dots & 0 \\ 0 & a & -2a + V_3 & a & 0 & \dots & 0 \\ 0 & 0 & a & -2a + V_4 & a & \dots & 0 \\ \vdots & \vdots & \vdots & \vdots & \vdots & \ddots & \vdots \\ 0 & 0 & 0 & 0 & 0 & \dots & -2a + V_{N-1} \end{pmatrix}, \quad \text{which uniquely}$$

determines the spectrum  $E_n$  and the wave function of each state  $\Psi_n$ .

Let us now consider a more realistic and complex mathematical model corresponding to the local region in Fig. 1a. For such a model, consideration of the boundary conditions (14) is mandatory. Using the finite-difference approximation for the first derivative in the form:

$$\frac{d}{dx} f(x_i) = f'(x) \approx \frac{f(x_i) - f(x_{i-1})}{\Delta} \quad (19)$$

we will have:

$$\begin{cases} \Psi_0 = \Psi_1; \\ \Psi_0 - 2\Psi_1 + \Psi_2 = 0; \end{cases} \quad \begin{cases} \Psi_{N-1} = \Psi_N; \\ \Psi_{N-2} - 2\Psi_{N-1} + \Psi_N = 0. \end{cases} \quad (20)$$

As a result, the difference scheme (17) is modified and takes on the following form:

$$\begin{pmatrix} V_1 & a & 0 & 0 & 0 & \dots & 0 \\ a & -2a + V_2 & a & 0 & 0 & \dots & 0 \\ 0 & a & -2a + V_3 & a & 0 & \dots & 0 \\ 0 & 0 & a & -2a + V_4 & a & \dots & 0 \\ \vdots & \vdots & \vdots & \vdots & \vdots & \ddots & \vdots \\ 0 & 0 & 0 & 0 & 0 & \dots & V_{N-1} \end{pmatrix} \begin{pmatrix} \Psi_1 \\ \Psi_2 \\ \Psi_3 \\ \Psi_4 \\ \vdots \\ \Psi_{N-1} \end{pmatrix} = E \begin{pmatrix} \Psi_1 \\ \Psi_2 \\ \Psi_3 \\ \Psi_4 \\ \vdots \\ \Psi_{N-1} \end{pmatrix}. \quad (21)$$

The algorithmic approach to solving the difference scheme (21) is similar to that of the difference scheme (18), it consists in finding the eigenvalues and eigenfunctions of the

$$A_{nm} = \begin{pmatrix} V_1 & a & 0 & 0 & 0 & \dots & 0 \\ a & -2a + V_2 & a & 0 & 0 & \dots & 0 \\ 0 & a & -2a + V_3 & a & 0 & \dots & 0 \\ 0 & 0 & a & -2a + V_4 & a & \dots & 0 \\ \vdots & \vdots & \vdots & \vdots & \vdots & \ddots & \vdots \\ 0 & 0 & 0 & 0 & 0 & \dots & V_{N-1} \end{pmatrix}.$$

#### 4. DEVELOPMENT OF SOFTWARE FOR IMPLEMENTING THE MATHEMATICAL MODEL OF THE SCHRÖDINGER EQUATION IN THE FORM OF A GRID PROBLEM

The software implementation of mathematical models of effective potentials as spectral problems for the stationary Schrödinger equation was carried out based on the constructed (18)–(21) grid finite difference schemes [19]. We started with the implementation of the simplest components of this software system block, namely for the potential model with infinitely high walls, within the potential well for which  $U(z)=0$ . The main parameters that can be changed in such a model are the electron's effective mass  $m$  and the width of the potential well  $L$ . We also took the number of divisions of the one-dimensional grid equal to  $N=500$ , which corresponds to a matrix (18) and (21) of size  $500 \times 500$ , while ensuring an accuracy of  $10^{-6}$ . The implementation of this component of the software system is presented in Fig. 2.

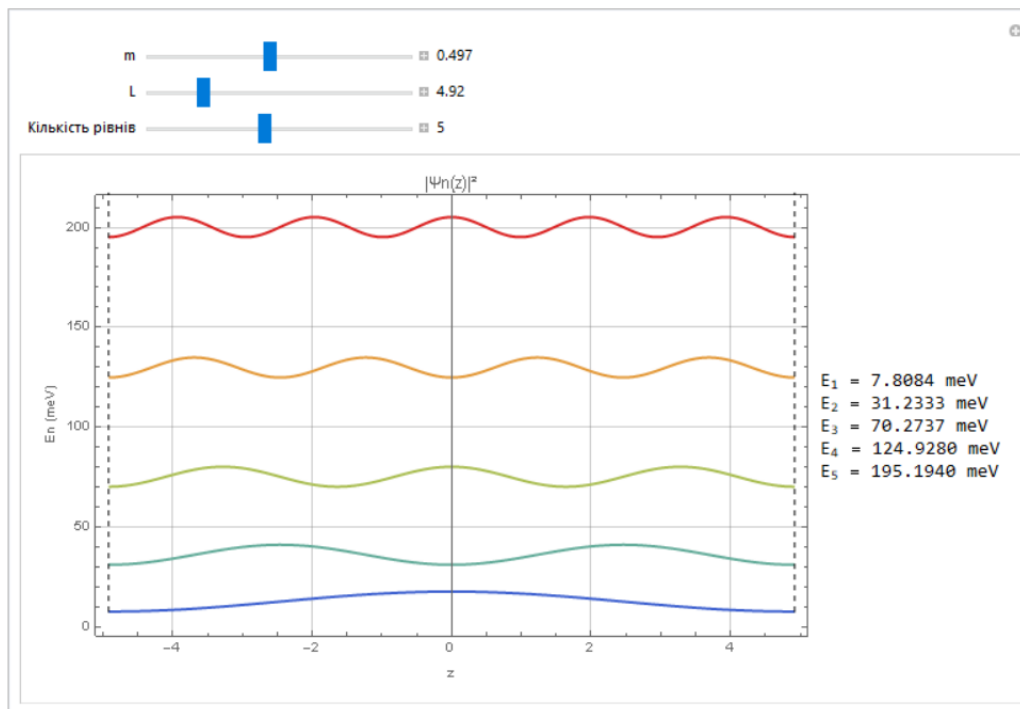


**Figure 2.** Modeling the spectrum and squared moduli of wave functions in a potential well with infinitely high walls

The possibility of continuous change in the electron's effective mass  $m$  and the width of the potential well  $L$  was implemented using sliders. The electron energy level number was also changed using a discrete-step spinner. For convenience, the squared moduli of the wave functions  $|\Psi_n(E_n, z)|^2$  are plotted on the energy scale, and the energies  $E_n$  themselves are displayed in a side menu.

Next, mathematical models for different effective potentials in a potential well with potential walls of finite height  $U_0$  were implemented. The component of the software system created based on the quantum oscillator model with  $U = kz^2/2$  is presented in Fig. 3a. In addition to the possibility of changing the electron's effective mass  $m$  and the width of the potential well  $L$  using sliders, and the number of electron levels with a discrete step, the possibility of changing the potential barrier height  $U_0$  and the effective stiffness  $a$  has also been implemented. Thus, in this implemented mathematical model, we can interactively change all its parameters.

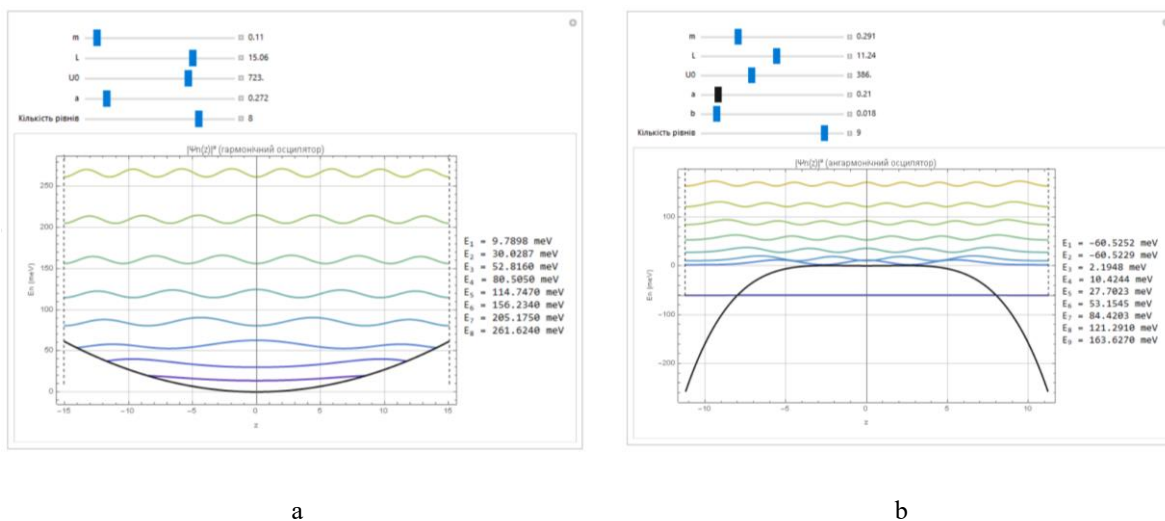


**Figure 3.** Modeling the spectrum and squared moduli of wave functions in a potential well with finite walls for a quantum harmonic oscillator (a) and quantum anharmonic oscillator (b)

A similar situation exists for the anharmonic oscillator for which  $U = az^2 + bz$ , the software implementation of which mathematical model is presented in Fig. 3b. Here, unlike the harmonic oscillator model discussed above, the possibility of changing the anharmonicity parameter  $b$  has also been implemented.

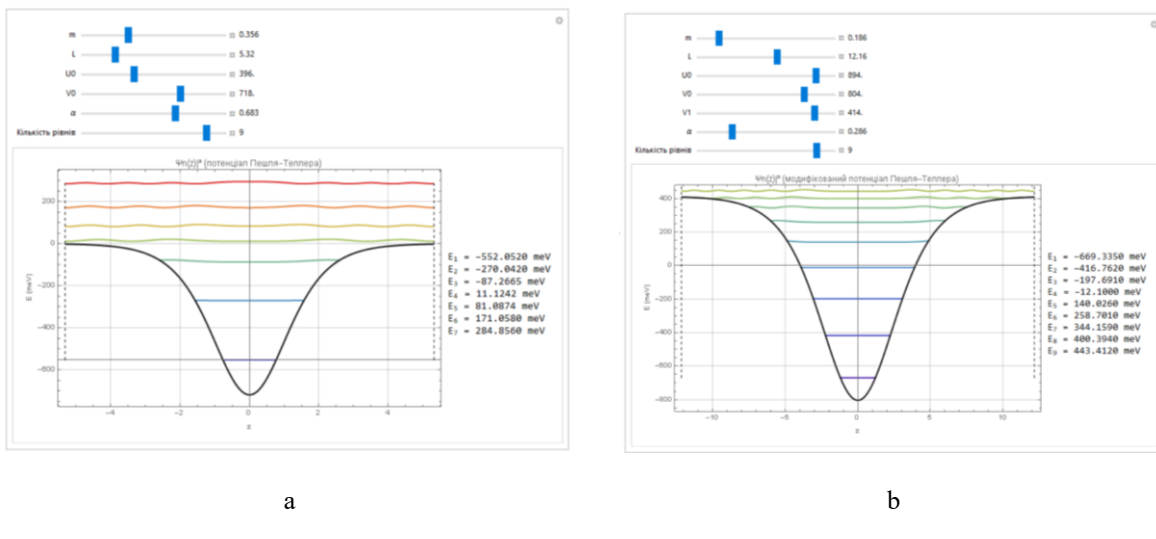


**Figure 4.** Modeling the spectrum and squared moduli of wave functions in a potential well with finite walls for the Pöschl-Teller potential (a) and modified Pöschl-Teller potential (b)

Next, the software implementation of the Pöschl-Teller potential was carried out:  $V(z) = -V_0 / \cosh^2(az)$ . Such a mathematical model is additionally characterized by the depth value  $V_0$  and the generalized width of the quantum well  $L$ . The results of such mathematical modeling in the form of a software block are presented in Fig. 4a.

Unlike the mathematical models of the harmonic and anharmonic oscillator, which are used in models of molecular spectra, the Pöschl-Teller potential is well suited for approximating potential traps for volatile hydrocarbons. One of the alternative options for mathematical models of potential traps is the modified Pöschl-Teller potential:  $V(z) = -V_0 / \cosh^2(az) + V_1 \tanh^2(az)$ . It has greater flexibility and reliability for modeling,

as this model contains an additional "fitting" parameter  $V_1$ . The results of the developed software block for such a mathematical model, with sliders available for changing all parameters, are presented in Fig. 4 b.

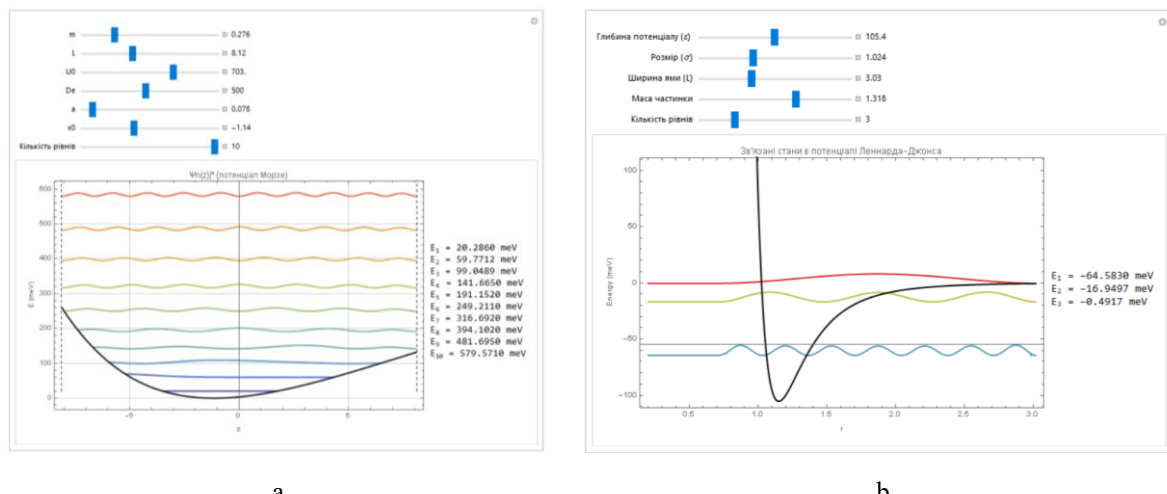


**Figure 5.** Modeling the spectrum and squared moduli of wave functions in a potential well with finite walls for the Morse potential (a) and Lennard-Jones potential (b)

For mathematical modeling of vibrational processes in diatomic molecules and often as potential traps for such molecules, the Morse potential is used:  $V(z) = D_e \left(1 - e^{-a(z-x_0)}\right)^2$ . In our generalized model, this potential is characterized by the following additional parameters: the depth of the potential well  $D_e$ , the effective width of the potential  $a$ , and the position of the minimum of the effective potential  $x_0$ . The component of the software system that provides effective mathematical modeling of the spectrum and squared moduli of wave functions works as shown in Fig. 5a. An important feature of the software block we have developed is the possibility of direct calculation of the spectrum and quantum transition energies, which allows determining the ionization energies and activation energies possible in both electronics and molecular dynamics.

The last component of the software system we have developed is the component that provides mathematical modeling of the Lennard-Jones potential:  $V(z) = 4\varepsilon \left[ \left(\frac{\sigma}{z}\right)^{12} - \left(\frac{\sigma}{z}\right)^6 \right]$ ,

where  $\varepsilon$  is the depth of the potential well, and  $\sigma$  is the distance at which the potential is zero. A feature of this potential is the partial states associated with the potential well at  $V(x) < 0$ . Transitions between these states determine the activation energy during the processes of molecule adsorption in functional materials with micropores. To fully solve this problem, it is necessary to algorithmically implement a model that allows for mathematical modeling of the mentioned energies with possible changes in all parameters of both the potential well and the Lennard-Jones potential itself. The result of the operation of such a component of the software system is presented in Fig. 5b.

## 5. CONCLUSIONS

1. This study presents a comprehensive analysis of the subject domain encompassing micro- and nanoelectronics, with a particular focus on applying software engineering methodologies and principles for the development and verification of mathematical models of

effective potentials. These potentials emerge during the simulation of quasiparticle states in mesoscopic structures. The study demonstrates the necessity of an integrated approach to implementing such mathematical models.

2. Ultimately, this approach is realized as a complex software system, where each software component is responsible for either visualizing the potentials or executing the core mathematical computations. As part of the practical outcomes, a range of mathematical models representing various types of effective potentials were developed. These models were visualized using the Wolfram Mathematica environment through specialized software modules that allow dynamic manipulation of key parameters. These modules constitute the first component of the developed software system.

3. The second component involves solving boundary value problems for the Schrödinger equation incorporating diverse effective potentials. Finite difference schemes were constructed based on these models and subsequently implemented in software. Each unit within this module facilitates the simulation of energy spectra, localization, and spatial distribution of quasiparticle states by enabling the modification of potential well parameters, effective potential properties, and relevant physical constants of the materials used.

4. A flexible and modular architecture was designed for the entire software system, ensuring intuitive access to both graphical and numerical results produced by each individual model. Owing to its versatility, the system can be applied not only in the field of electronics but also in adjacent and interdisciplinary domains. These include applications involving microporous materials, particularly in air purification systems and the monitoring of hazardous emissions into the atmosphere.

## References

1. Wang S., Zhou X., Zheng J. (2025) Optimization of GeSn nanostructures via tuning of femtosecond laser parameters. *Appl. Surf. Sci.*, vol. 679, pp. 161153. <https://doi.org/10.1016/j.apsusc.2024.161153>
2. Li K., Wang C., Sun L. (2024) Laser-assisted electrohydrodynamic jet printing of hierarchical nanostructure. *Appl. Therm. Eng.*, vol. 253, pp. 123659. <https://doi.org/10.1016/j.applthermaleng.2024.123659>
3. Labis J. P., Albritthen H. A., Shar M. A. (2024) Synthesis of Sn-ZnO nanostructures on MgO<0001> by hybrid pulsed laser ablation and RF magnetron sputtering tandem system for CO gas-sensing application. *J. Saudi Chem. Soc.*, vol. 28, pp. 101941. <https://doi.org/10.1016/j.jscs.2024.101941>
4. Liu J., Jiang Q., Yan J., Geng J., Shi L. (2024) Femtosecond pulse train-facilitated periodic nanostructuring on TiN films via laser-oxidation. *Opt. Laser Technol.*, vol. 177, pp. 111189. <https://doi.org/10.1016/j.optlastec.2024.111189>
5. Solana I., Chacon-Sanchez F., Garcia-Lechuga M., Siegel J. (2024) Versatile femtosecond laser interference patterning applied to high-precision nanostructuring of silicon. *Opt. Laser Technol.*, vol. 179, pp. 111360. <https://doi.org/10.1016/j.optlastec.2024.111360>
6. Cao K., Ye W., Zhang Y. (2024) Fabrication of multifunctional Co<sub>x</sub>N co-doped UIO-rGO aerogel with properties of hydrophobic, anti-corrosion, heat insulation, infrared stealth and electromagnetic wave absorption. *Chem. Eng. J.*, vol. 492, pp. 152275. <https://doi.org/10.1016/j.cej.2024.152275>
7. Ling Z., Chen J., Li S. (2024) A multi-band stealth and anti-interference superspeed light-guided swimming robot based on multiscale bicontinuous three-dimensional network. *Chem. Eng. J.*, vol. 485, pp. 150094. <https://doi.org/10.1016/j.cej.2024.150094>
8. Zhang Y., Zhang G., Wang C. (2024) The construction of structural defects in MoAlB thin films by leveraging the enhanced Kirkendall effect for improved infrared stealth performance. *Ceram. Int.*, vol. 50, pp. 21175–21183. <https://doi.org/10.1016/j.ceramint.2024.03.226>
9. Zanata S. M., El-Shafai N. M., Beltagi A. M. (2024) Bio-study: Modeling of natural nanomolecules as a nanocarrier surface for antioxidant and glucose biosensor. *Int. J. Biol. Macromol.*, vol. 264, pp. 130634. <https://doi.org/10.1016/j.ijbiomac.2024.130634>
10. Feugang J. M., Ishak G. M., Eggert M. W. (2022) Intrafollicular injection of nanomolecules for advancing knowledge on folliculogenesis in livestock. *Theriogenology*, vol. 192, pp. 132–140. <https://doi.org/10.1016/j.theriogenology.2022.08.032>
11. Li X., Wu M., Wang J. (2019) Ultrasmall bimodal nanomolecules enhanced tumor angiogenesis contrast with endothelial cell targeting and molecular pharmacokinetics. *Nanomedicin*, vol. 15, pp. 252–263. <https://doi.org/10.1016/j.nano.2018.10.004>
12. Santailler J. L., Duffar T., Théodore F. (1997) Some features of two commercial softwares for the modeling of bulk crystal growth processes. *J. Cryst. Growth*, vol. 180, pp. 698–710. [https://doi.org/10.1016/S0022-0248\(97\)00313-8](https://doi.org/10.1016/S0022-0248(97)00313-8)

13. Leng D., Li P., Kong F. (2024) Experimental and numerical study on single ice crystal growth of deionized water and 0.9% NaCl solution under static magnetic field. *Int. J. Refrig.*, vol. 168, pp. 297–306. <https://doi.org/10.1016/j.ijrefrig.2024.09.005>
14. NextNano Software. URL: <https://www.nextnano.de/products/overview.php>
15. NEMO-3D. URL: <https://engineering.purdue.edu/gekcogrp/software-projects/nemo3D/>
16. Cooper J. D., Valavanis A., Ikonić Z., Harrison P., Cunningham J. E. (2010) Finite difference method for solving the Schrödinger equation with band nonparabolicity in mid-infrared quantum cascade lasers. *J. Appl. Phys.*, vol. 168, pp. 297–306. <https://doi.org/10.1063/1.3512981>
17. Wang W., Hwang T.-M., Lin W.-W., Liu J.-L. (2003) Numerical methods for semiconductor heterostructures with band nonparabolicity. *J. Comput. Phys.*, vol. 108, pp. 113109. [https://doi.org/10.1016/S0021-9991\(03\)00268-7](https://doi.org/10.1016/S0021-9991(03)00268-7)
18. Xue T., Yang Y., Yu D., Wali Q. (2023) 3D Printed Integrated Gradient-Conductive MXene/CNT/Polyimide Aerogel Frames for Electromagnetic Interference Shielding with Ultra-Low Reflection. *Nano-Micro Lett.*, vol. 15, p. 45. <https://doi.org/10.1007/s40820-023-01017-5>
19. Boiko I., Petryk M., Mykhalyk D. (2017) Model of nanoporous medium with charged impurities // *Sci. J. TNTU*, vol. 87, no. 3, pp. 134–138. [https://doi.org/10.33108/visnyk\\_tntu2017.03.134](https://doi.org/10.33108/visnyk_tntu2017.03.134)

**УДК 5004.942, 519.635, 519.642, 519.673, 519.652**

## **ПРОГРАМНА СИСТЕМА ДЛЯ МАТЕМАТИЧНОГО МОДЕЛЮВАННЯ ВПЛИВУ ЕФЕКТИВНИХ ПОТЕНЦІАЛІВ НА ЕЛЕКТРОННІ СТАНИ У КВАНТОВИХ ЯМАХ**

**Ігор Бойко; Софія Хемій**

*Тернопільський національний технічний університет імені Івана Пуллюя,  
Тернопіль, Україна*

**Резюме.** Представлено розгорнутий огляд сучасного стану досліджень та аналіз математичних моделей, які використовуються для описування електронних процесів у низьковимірних структурах, зокрема у квантових ямах. Особливу увагу приділено розробленню програмних рішень, що забезпечують точне та ефективне математичне моделювання спектральних характеристик електронних станів із застосуванням широкого спектру ефективних потенціалів. У межах дослідження розроблено архітектуру програмного комплексу, який поєднує в собі функціональність для виконання обчислювальних експериментів, зміни параметрів моделей та візуалізації результатів. Розглянуто такі типи ефективних потенціалів, як гармонійний осцилятор, ангармонійний осцилятор, потенціал Пешиля–Теллера, модифікований потенціал Пешиля–Теллера, потенціал Морзе, потенціал Леннарда–Джонса. Ці потенціали широко застосовуються в квантовій механіці для описування взаємодії частинок у системах з обмеженнями розмірності. Реалізовані в програмному середовищі алгоритми дозволяють користувачам змінювати фізичні параметри (наприклад, масу частинок, глибину потенціальної ями, її ширину), а також геометричні характеристики системи, що моделюється, відповідно до конкретного типу наноструктури чи матеріалу. Однією з ключових особливостей програмного комплексу є зручний інтерфейс для інтерактивної побудови графіків ефективних потенціалів та спектральних ліній електронних станів. Система також забезпечує чисельне розв'язання відповідних рівнянь Шредінгера з урахуванням вхідних параметрів і генерацією результатів у вигляді графіків, таблиць та інших форматів, придатних для подальшого аналізу. Важливим етапом стало тестування працездатності комплексу на основі прикладів реальних фізичних систем і порівняння отриманих результатів із теоретичними прогнозами та літературними даними. Завдяки модульній структурі, програмний комплекс може бути розширеній новими моделями або адаптований до інших типів потенціалів та умов. У підсумку, створена програмна система є універсальним інструментом для дослідників і розробників, які працюють у галузі мікро- та наноелектроніки, оскільки дозволяє не лише проводити точні розрахунки спектральних характеристик електронних станів у квантових ямах, але й служити освітнім та науковим засобом для вивчення поведінки електронів у різних потенціальних конфігураціях.

**Ключові слова:** математична модель, програмна система, *Wolfram Mathematica*, квантова яма, метод скінчених різниць, ефективні потенціали.

[https://doi.org/10.33108/visnyk\\_tntu2025.03.115](https://doi.org/10.33108/visnyk_tntu2025.03.115)

Отримано 30.07.2025